Available online at www.sciencedirect.com

Journal of Photochemistry and Photobiology A: Chemistry 162 (2004) 329–338

Journal of Photochemistry and Photobiology A:Chemistry

www.elsevier.com/locate/jphotochem

Novel and efficient dye-linked radical generators for visible light photoinitiating polymerization

Koichi Kawamura*

Yoshida-Minami Factory, Fuji Photo Film Co., Ltd., 4000 Kawashiri Yoshida-cho, Haibara-gun, Shizuoka 421-0396, Japan

Received 15 June 2003; received in revised form 17 August 2003; accepted 28 August 2003

Abstract

Dye-linked initiators consisting of a benzothiazolylidene-rhodanine merocyanine dye (M) and a substituted bis(trichloromethyl)-1,3,5-triazine initiator (T) linked by a different number of methylene units and at different positions were prepared in order to reveal the effect of the structure of linked systems on the efficiency of photopolymerization. The spectroscopic studies clearly showed that the dye-linked initiators exhibit a marked increase in the efficiency of photobleaching and fluorescence quenching compared to a simple mixture of the dye/initiator and that the efficiency among the linked systems is dependent on the number and position of methylene units. These results are reasonably explained in terms of the efficiency of electron transfer between the dye and the initiator, which eventually results in the formation of a radical. The relative photoinitiating efficiency of dye-linked initiators in photopolymerization of acrylates was also evaluated and the trends observed for polymerization are essentially the same as that observed spectroscopically.

Keywords: Polymerization; Photoinitiation; Radical; Sensitization; Merocyanine; Electron transfer

1. Introduction

Many attempts have been made to develop efficient photoinitiating polymerization systems that can be used upon visible light excitation since such systems are expected to have wide applications in typical practical fields, such as high-speed photopolymers in computer-to-plate laser imaging and three-dimensional polymerization systems. It seems rather difficult to develop initiators that generate an initiating radical by a bond cleavage upon direct excitation (type I) with a visible light. On the other hand, multi-components photoinitiating systems employing a dye as a visible-light absorber look more promising. In these systems, the photophysical energy transfer from the excited state of the dye to the second component that is supposed to yield a free radical is generally not favored in view of energetic relationship between the dye and the initiating part. Instead of an energy transfer process, a photoinduced electron transfer process plays an important role in such systems. This process involves the use of light to initiate electron transfer from a donor (dye) to an acceptor (initiating part) molecule. These systems include aromatic ketone–amine combinations, dye–coinitiator pairs, as well as certain organometallic photoinitiators. Electron transfer processes in photopolymerization and imaging processes have recently been reviewed [1–8].

It is generally accepted that the rate of the electron transfer K_{et} depends not only on the free-energy change but also on the distance between donor and acceptor. The relationship between K_{et} and donor–acceptor separation R_{DA} has been well studied theoretically and experimentally, and indicates the sharp fall of K_{et} as donor and acceptor are separated by more than one or two classical collisional diameters [9–11].

Dye-linked photoinitiators, in which a radical generating part is brought close to a photosensitizing dye chromophore by a covalent bond, have been shown to be very useful as free-radical sources. However, the details of photo-processes of those systems are not clear, even though a large number of patents and papers dealing with dye-linked photoinitiator systems have appeared [12–19].

In order to investigate these issues, we have prepared several dye-linked photoinitiating systems and investigated their photochemical behaviors. The role of those new initiators in standard acrylate compositions was also examined. We chose a benzothiazolylidene-rhodanine merocyanine (M) as a sensitizer and a substituted bis(trichloromethyl)-1,3,5-triazine (T) as a radical generator, because the merocyanine dye have absorption maximum in a wavelength region corresponding to an emitting laser and the substituted

---

* Tel.: +81-548-32-7314; fax: +81-548-32-3919.
E-mail address: kawa@yoshis.fujifilm.co.jp (K. Kawamura).

1010-6030/$ – see front matter © 2004 Elsevier B.V. All rights reserved.
doi:10.1016/j.nainr.2003.08.013

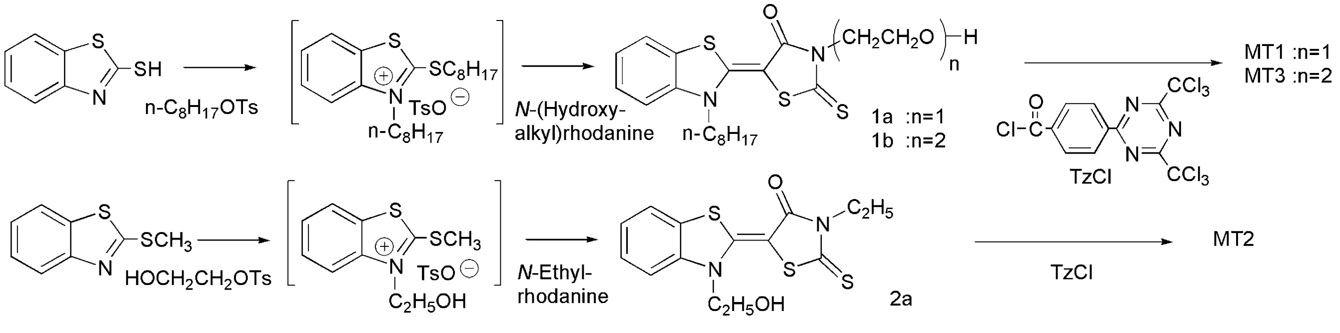

Scheme 1.

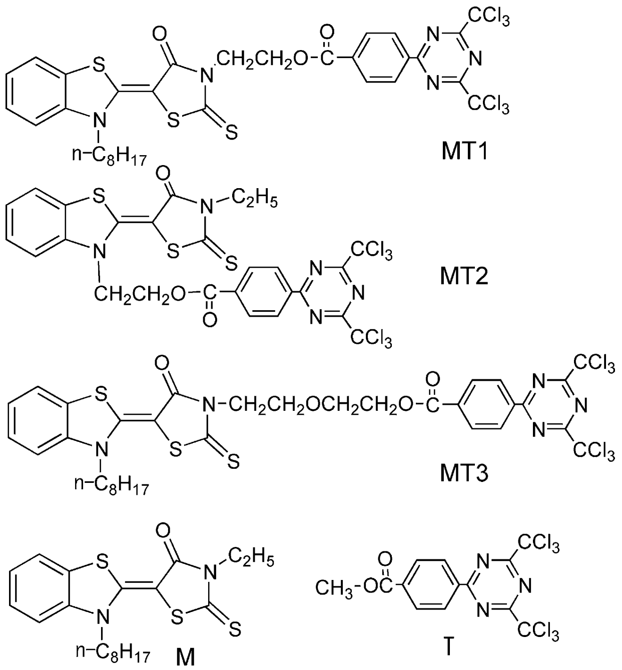

Fig. 1. Dye-linked initiators (MT1, MT2 and MT3) and reference compounds (M, T).

bis(trichloromethyl)-1,3,5-triazine derivatives (T) are widely employed as coinitiators in sensitized photopolymerization systems [20–24]. For this purpose, the following new photoinitiators (Fig. 1) were prepared, in which a merocyanine chromophore and a bis(trichloromethyl)-1,3,5-triazine chromophore were linked by a different number of methylene chains (MT1, MT3) and at different positions (MT1, MT2) (Scheme 1).

2. Experimental

2.1. General methods

Melting points were recorded on a Buch melting-point apparatus B540 and not corrected. ^{1}H NMR spectra were measured on a Varian Gemini-300. Mass spectra (EI-mass) were obtained on a JEOL JMS-600H. Steady-state absorption spectra in the UV-Vis regions were measured on a Carry-5 spectrophotometer. Fluorescence measurements were recorded using a Fluorolog-3 (Jobin Yvon Inc.) fluorometer. Solutions for measurements were deoxygenated by bubbling nitrogen for 10 min. Fluorescence spectra of films were monitored with front-face detection on coatings with absorbance values not more than 0.15 absorbance units. Double-bond conversion was monitored by using a FT-720 FT-IR Horiba spectrophotometer. We used the semi-empirical MOPAC package in the PM3/ZINDO approach to calculate the electronic transitions and the CONFLEX method in CaChe® system for searching low-energy conformations of the linked compounds. The *E* configuration around the C(2)=C(5′) bond between the benzothiazole nucleus and the rhodanine nucleus in the merocyanine dye was assumed, which was supported by a single-crystal X-ray determination [25]. HPLC analysis was performed on a Shimadzu Class-VP equipped with a diode array detector and eluted with acetonitrile/water in a volume ratio of 90:10.

2.2. Film preparation

Films for the measurement of photophysical behavior and photopolymerization were typically prepared in the following manner. The photoinitiator (a merocyanine/triazine combination or a linked initiator), a polyfunctional acrylate monomer (pentaerythritol tetraacrylate; Shin-Nakamura Chemical) and a polymeric binder (copolymers of methacrylic acid and benzyl methacrylate; mole ratio 20/80, Mw $=$ 24,000) were dissolved in a 1:1 (w/w) mixture of solvent (methylethyl ketone/1-methoxy-2-propanol), and the solution was cast on a glass or on a grained-surface aluminum plate. The solvent was evaporated with heating at 100 °C for 1 min. The thickness of the film thus prepared was about 2 μm. A thin layer of polyvinyl alcohol was over-coated onto the film to prevent the diffusion of atmospheric oxygen.

2.3. Measurement of photosensitivity

The light source was a 0.5 kW xenon lamp (Ushio Electric Instruments, UI 501C) and band-pass filters (Kenko Co. Ltd) were used to irradiate merocyanine alone in all irradiation experiments ($\lambda = 430$ nm). The kinetics of the polymerization was measured by following the disappearance of the IR absorption of the acrylic double bond at 807 cm^{-1} (CH_2=CH twisting, out of plane) or 1409 cm^{-1} (CH_2=CH twisting, in plane). The percentage of conversion was calculated from the decrease of the area of the IR absorption peak at 1409 cm^{-1} of the sample after exposure.

2.4. Materials

All solvents and chemicals were of reagent grade quality, obtained commercially and used without further purification. Pentaerythritol tetraacrylate (PET4A) are supplied by Shin-Nakamura Chemical and used as received.

2.4.1. Copolymer BA

The copolymer of methacrylic acid and benzyl methacrylate (mole ratio 20/80), abbreviated as BA, was synthesized by heating a monomer mixture in the presence 2,2′-azobis(2,4-dimethylvaleronitrile) at 65 °C and purified by repeated precipitation in methanol. GPC: Mw = 24,000.

2.4.2. Compound M (3-ethyl-5-(3-octyl-3H-benzothiazol-2-ylidene)-2-thioxo-thiazolidin-4-one)

A mixture of 2-mercaptobenzothiazole (5.0 g, 30 mmol) and *n*-octyl *p*-toluenesulfonate (25.7 g, 90 mmol) were heated with stirring at 150 °C for 4 h. Upon cooling to room temperature, *N*-ethyl rhodanine (4.83 g, 30 mmol) and triethylamine (7.07 g, 70 mmol) in ethanol (50 ml) was added and the mixture was heated to reflux for 30 min to give the yellow flocculent which precipitated from the solution. The mixture was then allowed to cool to room temperature, and the precipitate was filtered and washed with ethanol. Recrystallized from ethanol; 6.2 g, 51%; mp 150 °C; ^{1}H NMR (300 MHz, $CDCl_3$) δ: 7.64 (d, $J = 7.5$ Hz, 1H), 7.44 (m, 1H), 7.29 (m, 1H), 7.20 (d, $J = 8.4$ Hz, 1H), 4.24 (m, 4H), 1.88 (m, 2H), 1.5 (m, 2H), 1.33 (m, 11H), 0.90 (t, $J = 7.0$ Hz, 3H). HRMS calcd. for $C_{20}H_{26}N_2OS_3$ (*m*/*e*) 406.1241, found 406.1207.

2.4.3. Compound **1*a*** (3-(2-hydroxyethyl)-5-(3-octyl-3H-benzothiazol-2-ylidene)-2-thioxo-thiazolidin-4-one)

1a was prepared in the same way as M, using *N*-(2-hyroxyethyl)-rhodanine instead of *N*-ethyl rhodanine. Recrystallized from ethanol; 43%; mp 167.0–168.5 °C; ^{1}H NMR (300 MHz, $CDCl_3$) δ: 7.65 (d, $J = 7.8$ Hz, 1H), 7.46 (m, 1H), 7.31 (m, 1H), 7.23 (d, $J = 8.4$ Hz, 1H), 4.48 (t, $J = 5$ Hz, 2H), 4.23 (t, $J = 8.4$ Hz, 2H), 3.99 (t, $J = 5$ Hz, 2H), 2.4 (br, s, 1H), 1.89 (q, $J = 8$ Hz, 2H), 1.51 (m, 2H), 1.43–1.23 (m, 8H), 0.90 (t, $J = 7.0$ Hz, 3H).

2.4.4. Compound **1*b*** (3-[2-(2-hydroxyethoxy)ethyl]-5-(3-octyl-3H-benzothiazol-2-ylidene)-2-thioxo-thiazolidin-4-one)

1b was prepared in the same way as **1a**, using *N*-[2-(2-hyroxyethoxy)ethyl]-rhodanine instead of *N*-(2-hyroxyethyl)-rhodanine. Recrystallized from ethanol; 21%.

2.4.5. Compound **2*a*** (3-ethyl-5-[3-(2-hydroxyethyl)-3H-benzothiazol-2-ylidene]-2-thioxo-thiazolidin-4-one)

2-Methylmercaptobenzothiazole (10.0 g, 55 mmol) and 2-hydroxyethyl *p*-toluenesulfonate (23.8 g, 110 mmol) were heated with stirring at 140 °C for 3 h. Upon cooling to room temperature, ethanol (100 ml), *N*-ethyl rhodanine (8.9 g, 55 mmol) and triethylamine (16.7 g, 165 mmol) were added successively, and the mixture was heated to reflux for 30 min. After standing in a refrigerator overnight, the resulting precipitate was filtered, washed with two 10 ml portions of ethanol, and sucked dry. Recrystallized from ethanol. Yellow crystal; 8 g, 10%; mp 270–271 °C; ^{1}H NMR (300 MHz, $CDCl_3$) δ: 7.92 (d, $J = 6.9$ Hz, 1H), 7.65 (d, $J = 7.8$ Hz, 1H), 7.49 (m, 1H), 7.34 (m, 1H), 5.2 (br, s, 1H), 4.48 (t, $J = 5.4$ Hz, 2H), 4.09 (q, $J = 7.2$ Hz, 2H), 3.83 (t, $J = 5.4$ Hz, 2H), 1.19 (t, $J = 7.2$ Hz, 3H).

2.4.6. Compound MT1

To a solution of **1a** (1.13 g, 2.7 mmol) and 4-(4-chlorocarbonylphenyl)-2,6-bis-(trichloromethyl)-*s*-triazine [26] (1.36 g, 3.0 mmol) (prepared by chlorination of 4-(4-carboxylphenyl)-2,6-bis-(trichloromethyl)-*s*-triazine with thionyl chloride) in THF (100 ml) was added 4-(*N*,*N*-dimethylamino)pyridine (0.73 g, 6.0 mmol) dropwise with stirring at room temperature. After stirring for 1 h, the reaction mixture was poured into water and extracted with ethyl acetate. The organic layer was washed with saturated NaCl aqueous solution, dried over anhydrous Na_2SO_4, and then the solvent was evaporated. Flash column chromatography on silica gel with hexane/ethyl acetate (2/1) as an eluent and subsequent recrystallization from ethyl acetate/hexane gave MT1 (1.2 g, 53%) as yellow crystal: mp 176–178 °C; ^{1}H NMR (300 MHz, $CDCl_3$) δ: 8.70 (d, $J = 9.0$ Hz, 2H), 8.23 (d, $J = 8.7$ Hz, 2H), 7.62 (d, $J = 7.8$ Hz, 1H), 7.44 (m, 1H), 7.29 (m, 1H), 7.21 (d, $J = 8.1$ Hz, 1H), 4.71 (m, 4H), 4.21 (t, $J = 8.1$ Hz, 2H), 1.87 (m, 2H), 1.5–1.2 (m, 10H), 0.89 (m, 3H); HRMS calcd. for $C_{32}H_{29}Cl_6N_5O_3S_3$ (*m*/*e*) 836.9563, found 836.9645.

2.4.7. Compound MT2

MT2 was prepared in the same way as described above from **2a** (0.217 g, 0.64 mmol) and 4-(4-chlorocarbonylphenyl)-2,6-bis-(trichloromethyl)-*s*-triazine (0.29 g, 0.64 mmol); yield 0.28 g, 60%; yellow crystal: mp 195.5–196.0 °C; ^{1}H NMR (300 MHz, $CDCl_3$) δ: 8.68 (d, $J = 9.0$ Hz, 2H), 8.03 (d, $J = 8.1$ Hz, 2H), 7.51 (d, $J = 7.8$ Hz, 1H), 7.43–7.26 (m, 3H), 4.76 (m, 4H), 4.23 (q, $J = 7.2$ Hz, 2H), 1.32 (t, $J = 7.2$ Hz, 3H); HRMS calcd. for $C_{26}H_{17}Cl_6N_5O_3S_3$ (*m*/*e*) 752.8687, found 752.8624.

2.4.8. Compound MT3

MT3 was prepared in the same way as described above from **1b** (1.4 g, 3.0 mmol) and 4-(4-chlorocarbonylphenyl)-2,6-bis-(trichloromethyl)-*s*-triazine (1.36 g, 3.0 mmol); yield 0.65 g, 24.5%; yellow crystal: mp 139–141 °C; ^{1}H NMR (300 MHz, $CDCl_3$) δ: 8.55 (d, $J = 9.0$ Hz, 2H), 8.17 (d,

$J = 8.1$ Hz, 2H), 7.49 (d, $J = 7.8$ Hz, 1H), 7.24 (m, 1H), 7.14 (t, $J = 7.2$ Hz, 1H), 7.01 (d, $J = 8.4$ Hz, 1H), 4.49 (t, $J = 4.8$ Hz, 2H), 4.43 (t, $J = 5.7$ Hz, 2H), 4.09 (t, $J = 8.1$ Hz, 2H), 3.99 (t, $J = 5.7$ Hz, 2H), 3.91 (t, $J = 4.5$ Hz, 2H), 1.82 (m, 2H), 1.5–1.2 (m, 10H), 0.90 (t, $J = 6.5$ Hz, 3H); HRMS calcd. for $C_{34}H_{33}Cl_6N_5O_4S_3$ (*m*/*e*) 881.9899 ($M + H^+$), found 881.9835.

2.4.9. *Compound A1 (3-ethyl-5-(3-octyl-3H-benzothiazol-2-ylidene)-2-oxo-thiazolidin-4-one)*

3-Ethyl-5-(3-octyl-3*H*-benzothiazol-2-ylidene)-2-ethylsulfanyl-4-oxo-4,5-dihydro-thiazolium tetrafluoroborate (1.04 g, 2 mmol), which was prepared according to the patent [27], was dissolved in the mixture of acetonitrile (15 ml) and water (2 ml). Triethylamine (0.4 g, 4 mmol) and silver nitrate (0.3 g) was added to the solution. After stirring at 50 °C for 3 h, the mixture was poured into 100 ml of water to gave the solid which was collected by filtration. Recrystallized from methanol; 0.3 g, 38%; pale orange crystal. mp 133.7–133.9 °C; ^{1}H NMR (300 MHz, $CDCl_3$) δ: 7.56 (d, $J = 7.8$ Hz, 1H), 7.38 (m, 1H), 7.22 (m, 1H), 7.12 (d, $J = 8.4$ Hz, 1H), 4.16 (t, $J = 8.4$ Hz, 2H), 3.85 (q $J = 7.0$ Hz, 2H),1.86 (m, 2H), 1.48–1.26 (m, 13H), 0.89 (t, $J = 6.9$ Hz, 3H); (λ_{abs}^{max}, nm (ε, 10^4 M^{-1} cm^{-1}), THF): 377 (4.33); HRMS calcd. for $C_{20}H_{26}N_2O_2S_2$ (*m*/*e*) 390.1435, found 390.1433.

3. Results and discussion

3.1. *Steady-state absorption spectra*

The absorption spectra of the initiator compounds in tetrahydrofuran (THF) at a concentration of 10^{-5} M are shown in Fig. 2. The absorption spectra of linked compounds (MT1, MT2 and MT3) were almost identical with that of an equimolar mixture of each component merocyanine and triazine (M + T). This indicates that there is no appreciable interaction between these two chromophores in the ground state. Similar results were observed when these compounds are integrated in a photopolymer film.

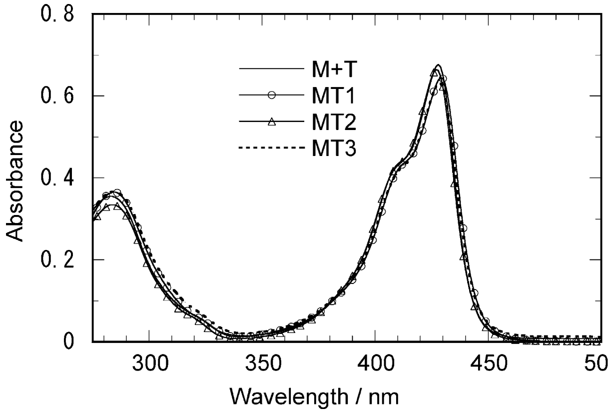

Fig. 2. Absorption spectra of MT1, MT2, MT3 and an equimolar mixture of merocyanine and triazine (M + T) in THF (1.0×10^{-5} M).

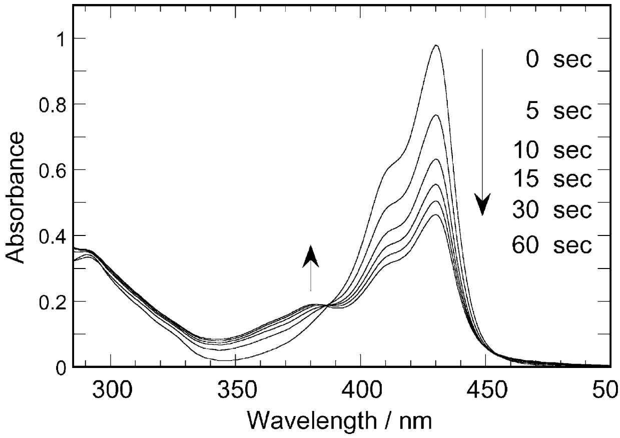

Fig. 3. Change of absorption spectra of MT1 upon irradiation at 430 nm in toluene.

3.2. *Steady-state photolysis*

The spectral change observed by steady-light irradiation of MT1 in deaerated toluene are shown in Fig. 3. When a solution of MT1 was irradiated with a light of 430 nm wavelength, where only the dye was excited, the band at 430 nm that is characteristic of the dye disappeared and a new band showing its maximum at 380 nm appeared, with an isosbestic point at 390 nm (Fig. 3). The new band at 380 nm is very similar with that of oxo-rhodanine dye (A1, see Scheme 2) and hence can be attributed to the oxo-rhodanine moiety presumably formed as a result of intramolecular electron transfer from the excited state of the dye. Similar spectral changes were observed under irradiation of other MT systems.

In marked contrast, similar irradiation of an equimolar mixture of the dye (M) and the triazine (T) showed essentially no change at least in the time range where appreciable

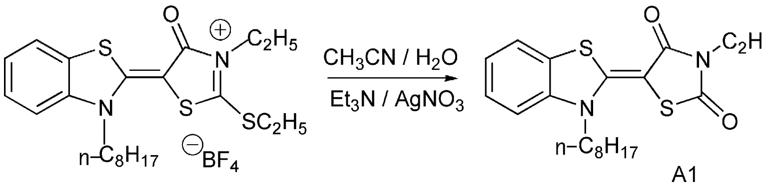

Scheme 2.

decay was noted for the linked system. The observations can be interpreted as indicating that MT1 undergoes intramolecular electron transfer reaction upon photoexcitation much faster than M + T system under these conditions.

The photoreactivity of linked photoinitiators in photopolymer coatings is of our major interest. In a photopolymerizable dry film system, which is generally a compatible mixture of a performed polymeric binder, a multifunctional acrylate monomer and a photoinitiating system, molecular diffusion is presumed to be severely restricted. Furthermore, a sensitizer and a coinitiator are loaded in high concentrations, typically 10–50 mmol/dm^3, in a thin film of about 1–5 μm thickness. Under these circumstances, different reactivity may be expected in a film than that in a fluid solution.

Thus, when the photopolymer coatings including initiators were irradiated at 430 nm, photobleaching was observed not only for MT1 system but also for M + T system, although photobleaching was apparently more efficient in the former. It is noted here that both systems showed a similar spectral change upon irradiation. This indicates that the same electron transfer reaction takes place in M + T system as in MT1 system in a photopolymer coating (Fig. 4).

In order to estimate the effect of the initiator structure on the efficiency of photobleaching, a series of initiators were irradiated in the photopolymer coating under essentially the identical conditions and the disappearance of the band at 430 nm was plotted as a function of the irradiation time (Fig. 5). This revealed that the decay of the linked initiators is much faster than the simple mixture of each component, suggesting a more efficient photochemical event. Among the linked systems, MT1 and MT2 decayed appreciably faster than MT3 system. Moreover, MT2 system decayed slightly faster than MT1 system even though both compounds have the same methylene units. This may indicate that the efficiency of electron transfer is dependent on the position where an acceptor is linked, which in turn may reflect the distance between a donor and an acceptor (see below).

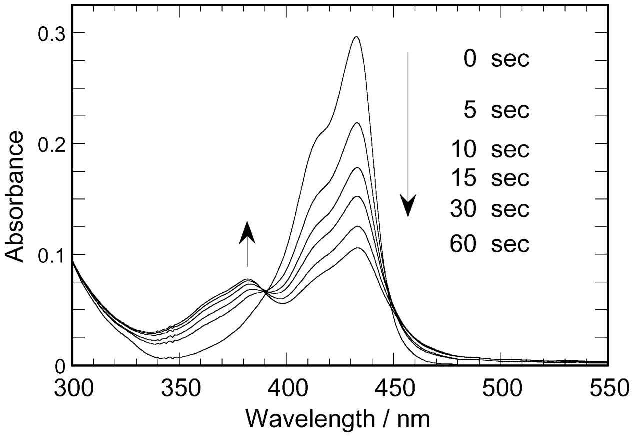

Fig. 4. Change of absorption spectra of MT1 (12 mmol/dm^3) in the photopolymer coatings, upon irradiation at 430 nm.

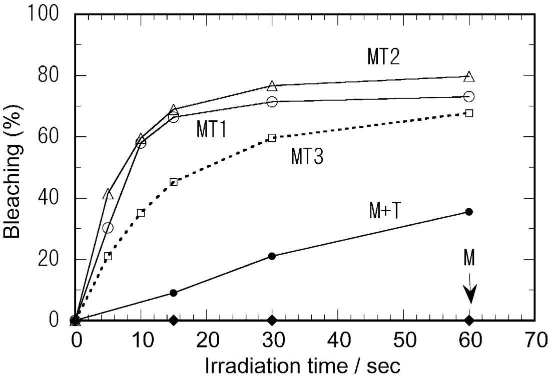

Fig. 5. Photobleaching (%) of the merocyanine chromophore as a function of time of the photopolymer coating films on irradiation at 430 nm: (●) M + T; (○) MT1; (△) MT2; (□) MT3. Concentration of photoinitiator (12 mmol/dm^3). Merocyanine alone (M) does not photobleach under these experimental conditions.

3.3. Fluorescence quenching experiments

The fluorescence spectra of the merocyanine and the linked compounds in THF at a concentration of 3×10^{-6} M are shown in Fig. 6. The fluorescence of merocyanine was not quenched at all by an equimolar solution of the triazine. In contrast to this, the fluorescence of the linked initiators is significantly weaker than that of merocyanine itself. Since the absorption spectra of the liked initiators are essentially the same with that of merocyanine, the decrease in the fluorescence intensity can be interpreted in terms of intramolecular quenching by the triazine part. Then, the fraction of quenching (quenching efficiency, %) is regarded as a measure of efficiency of intramolecular interaction between the merocyanine and the triazine parts. This increases in the order of MT3 (20%), MT1 (37%), and MT2 (51%), indicating that the longer methylene compound (MT3) shows less efficient quenching than the shorter methylene compounds (MT1 and MT2). It is interesting to note that the fraction of quenching is larger in MT2 than MT1. This may be due

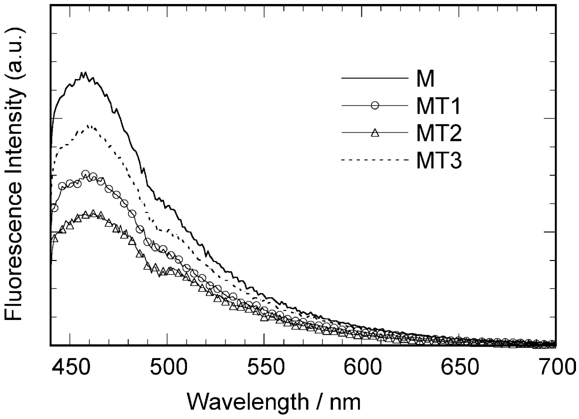

Fig. 6. Emission spectra of the compounds (3×10^{-6} M) in THF at room temperature: (—) M; (○) MT1; (△) MT2; (· · ·) MT3. Excitation: 430 nm.

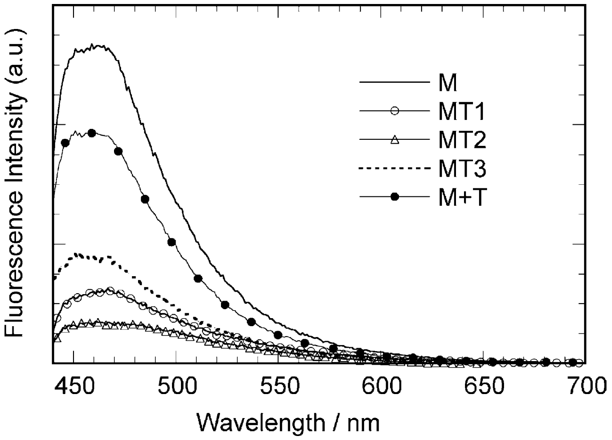

Fig. 7. Emission spectra of the compounds (12 mmol/dm^3) in a photopolymer matrix at room temperature: (—) M; (●) M + T; (○) MT1; (△) MT2; (···) MT3. Excitation: 430 nm.

to the favorable donor–acceptor orbital interaction in MT2 upon intramolecular electron transfer.

Fluorescence spectra were also measured in photopolymer coating films (Fig. 7), where the intensity of fluorescence decreased in the same order as in solution runs. Thus, the linked compounds (MT1, MT2 and MT3) shows decreased fluorescence as opposed to the unlinked pairs (M + T), most probably due to intramoleculer quenching. The quenching efficiency is largest in MT2 among the photoinitiating systems. The trend in the efficiency of photobleaching shown in Fig. 5 is in accord with that of fluorescence quenching. This suggests that the photobleaching reaction takes place via an intramolecular electron transfer reaction from the singlet excited state of the dye chromophore to the initiator chromophore.

3.4. Energetics of electron transfer

The free-energy change for electron transfer from an excited donor D to an acceptor A in the ground state is expressed by the Rehm–Weller equation [28]:

$$\Delta G^\circ = E(\mathrm{D}/\mathrm{D}^{\bullet +}) - E(\mathrm{A}^{\bullet -}/\mathrm{A}) - E(\mathrm{S}_1) - \frac{e^2}{\varepsilon R_{\mathrm{DA}}} \qquad (1)$$

where $E(\mathrm{S}_1)$ is the excited-state energy of the donor (merocyanine in this case), $E(\mathrm{D}/\mathrm{D}^{\bullet +})$ the oxidation potential of the donor, and $E(\mathrm{A}^{\bullet -}/\mathrm{A})$ the reduction potential of the acceptor (triazine in this case). The last term accounts for the Coulomb energy associated with the separation of charges in the electron transfer products. This factor has been ignored in this work.

The free-energy change of the present system can be estimated to be −0.93 eV by using the oxidation potential of the merocyanine (+0.83 V versus SCE), the excitation energy of the merocyanine (2.70 eV), and the reduction potential of the triazine (−0.94 V versus SCE) [29]. This value is rather large compared to that of other related reactions. For instance, the photoinduced electron transfer reaction from light-absorbing Rose Bengal to the triazine has been reported, and the free-energy change of electron transfer was estimated to be −0.6 eV [29]. In our merocyanine/triazine system, the free-energy change of electron transfer is larger than that of Rose Bengal/triazine system. This also supports the idea that electron transfer is a likely mechanism.

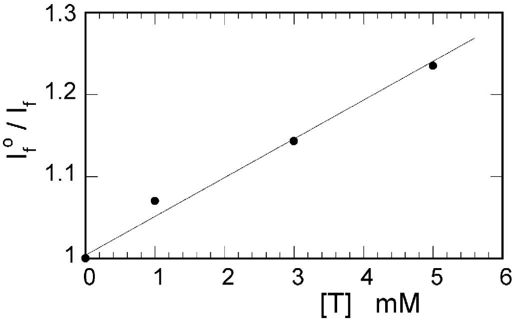

Fig. 8. Stern–Volmer plot for the quenching of the fluorescence of merocyanine (3×10^{-6} M) by triazine in nitrogen-saturated THF. Excitation: $\lambda = 430$ nm.

In accordance with this large negative free-energy change for electron transfer, the fluorescence of the merocyanine dye was quenched by the triazine at high concentrations (>0.001 M) in THF. The results obtained from fluorescence-quenching spectra were treated with the Stern–Volmer equation (Fig. 8). The Stern–Volmer constant k_{sv} is estimated to be 49 M^{-1} from the slope. Assuming the fluorescence lifetime to be 0.4 ns based on that of MC540 [30], the rate constant of fluorescence quenching k_{q} is estimated to be $1.2 \times 10^{11}\ \mathrm{M}^{-1}\,\mathrm{s}^{-1}$. This large quenching constant is in agreement with the large negative free-energy change for electron transfer.

The issues of electron transfer in a matrix have received extensive attention both from the theoretical and practical points of view [31–35]. Electron transfer is also a fundamental process in dye-sensitized photoinitiation in photopolymerizing systems, and many studies of fluorescence quenching have been reported in a polymer matrix [6–8,36]. If the fluorescent and quenching molecules do not change their positions during the lifetime of the fluorescent molecule, the fluorescence intensity of the molecules is expressed by the Perrin equation:

$$\frac{I_0}{I} = \exp(NV[\mathrm{Q}]) \qquad (2)$$

where I_0 is the emission intensity in the absence of a quencher, I the observed emission intensity, N the Avogadro's number, [Q] the concentration of a quencher, and V the volume of the "quenching sphere."

Thus, the quenching of the merocyanine fluorescence by various concentrations of the triazine quencher in photopolymer films was analyzed by this equation. The data fit Eq. (2) reasonably well as shown in Fig. 9, which demonstrates the total inhibition of diffusion in these systems. From the slope of this plot, the "active-quenching radius," R_{q}, can be estimated to be about 13 Å. This short distance is reasonable

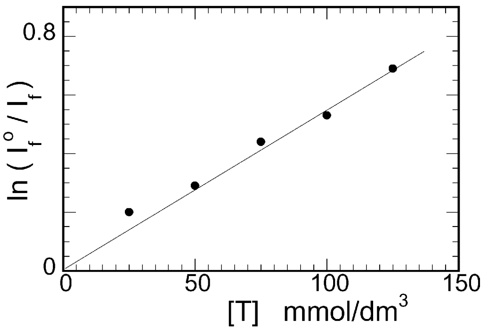

Fig. 9. Perrin plot for the fluorescence quenching of merocyanine by triazine in photopolymer films. Excitation: λ = 430 nm.

for the quenching by the electron transfer process. Moreover, the dependence of the quenching radius (R_q) on the free energy for the electron transfer quenching process in a polymer solid matrix has been illustrated by several authors, and the quenching radius of 13 Å is not inconsistent with the reported values [36–39]. Rather short quenching radius of 13 Å also indicates that the excited state of the dye is quenched only by the molecule of triazine, which is located in very close proximity. In other words, if the triazine is outside the quenching radius of the dye, the excited state of the dye will not be quenched at all. Thus, the donor–acceptor distance is a crucial factor for determining the efficient electron transfer in a photopolymer coating.

In unlinked photoinitiating systems, in which the donor and the acceptor were separated by about 25 Å at a concentration of 24 mmol/dm^3 in a photopolymer coating film, efficient electron transfer from the excited merocyanine to the triazine would not occur because they are outside the quenching sphere at this concentration [9].

In contrary to this, in linked donor–acceptor systems, the donor–acceptor distance can be adjusted by choosing the number of a methylene unit, and it is easy to link the donor and the acceptor within the quenching radius so as to cause the efficient electron transfer reaction. The accurate estimation of the donor–acceptor distance in MT1, MT2 and MT3 is difficult partly due to their flexible nature of methylene chains, but rough estimate using MM2 calculation suggests that the donor–acceptor separation in MT3 is less than 19 Å. The even more shorter separation would be expected in the shorter methylene MT1 and MT2. Thus, the donor–acceptor separation in our linked donor–acceptor systems is obviously shorter than that of the unlinked pair and the observed efficient quenching in linked compounds would reasonably be explained by this quenching radius.

3.5. Product analysis of the photoirradiated photopolymer coatings containing unlinked dye/triazine as an initiating system

In order to achieve a deeper insight into the possible mechanism of electron transfer in the photopolymerization system, the photopolymer coating film containing the equimolar mixture of the dye and the triazine was irradiated, and the photodecomposition products were identified by extracting the photoirradiated coating mixture with acetone, followed by analysis of the extracts by HPLC equipped with a diode array UV-Vis detector. The products were determined by comparing the retention time and UV-Vis absorption spectrum with that of the authentic samples. HPLC showed two new products P1 and P2. The UV-Vis absorption spectra of P1 and P2 were shown in Fig. 10 together with those of starting materials. The new product P2 was tentatively assigned as a photodecomposition product derived from the triazine, because its UV spectrum was similar to that of the starting triazine. The product P1 showing absorption maximum at 378 nm was identical in its retention time and in its spectral features with that of authentic oxo-rhodanine (A1) which was synthesized by a non-photochemical synthetic route as shown in Scheme 2.

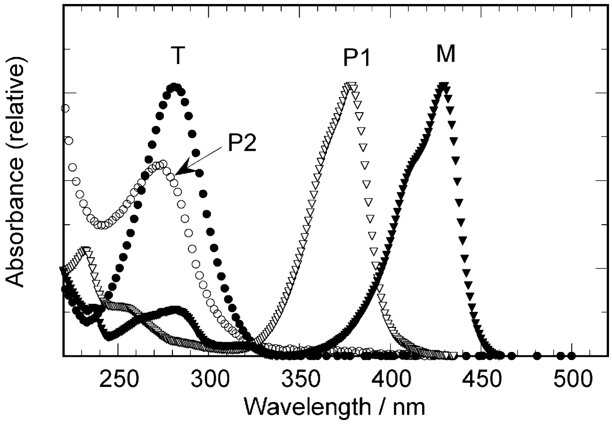

Fig. 10. UV-Vis absorption spectra of photoproducts, P1 and P2. The spectra were monitored by a diode array detector in HPLC. The absorption spectra of M and T were shown for comparison.

3.6. Possible mechanism for electron transfer

All the results of this investigation into the fluorescence quenching experiments and products analysis reveal the possible mechanism of a radical generation in the photolysis of triazine (T) in the presence of merocyanine dyes (M) as shown in Scheme 3. According to this mechanism, the electron transfer takes place from excited state of M to T to generate merocyanine cation radical ($M^{\bullet +}$)/triazine anion radical ($T^{\bullet -}$) pairs. The latter then could form a chloride anion and a triazine radical, which enters into the polymerization reaction and the former can decompose to give oxo-rhodanine (A1) via hydrogen abstraction, followed by hydrolysis. The present mechanism is reasonable in view of the analogues dye/triazine photosensitization mechanism which was reported by Sciano and co-workers [20].

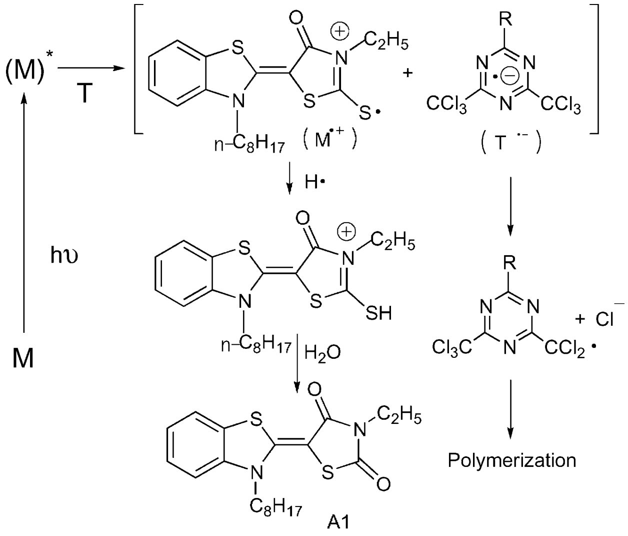

Scheme 3. Proposed mechanism of radical generation and photobleaching reaction in a photopolymer film.

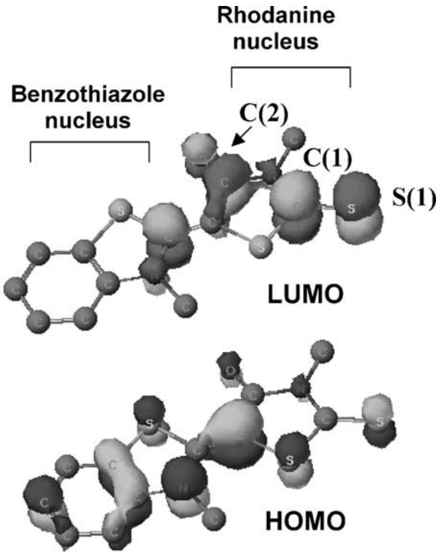

Fig. 11. Molecular orbitals of the merocyanine dye as calculated by ZINDO method.

3.7. MO considerations

All the experimental observations thus far obtained clearly indicate that photoreactivity of the linked initiators is significantly dependent on the structure. Thus, the reactivity of MT3 with a longer tethering chain is found to be much less than that of MT1 and MT2 with a shorter chain. This result could be reasonably explained on the basis of the donor–acceptor distance in the intramolecular electron transfer reaction. Furthermore, there is a slight difference in the sensitivity between MT2 and MT1; the former shows a higher rate of photobleaching (Fig. 5) and a more efficient fluorescence quenching (Figs. 6 and 7). The major difference between the two systems is the position to which the triazine is connected to the dye. The reason for the enhanced interaction in MT2 is not clear at present, but this effect may be attributable to the more effective orbital interaction between the triazine moiety and the photoexcited sensitizing moiety in MT2 system, compared to that in MT1 system.

ZINDO calculations indicate that the absorption at 430 nm in merocyanine corresponds to the transition from HOMO to LUMO level. This transition corresponds to intramolecular charge transfer from a benzothiazole nucleus to a rhodanine nucleus in merocyanine, which leads to large negative charges localized in a rhodanine nucleus in its excited state (Fig. 11). Thus, it is reasonable to assume that, when merocyanine is irradiated into its excited state, electron transfer to the triazine part takes place from the electron rich rhodanine nucleus rather than from the benzothiazole nucleus in the merocyanine molecule. Therefore, for the effective orbital interaction to take place, it is important to shorten the distance between the rhodanine nucleus and the triazine nucleus rather than that between the benzothiazole nucleus and the triazine in this linked photoinitiating system.

From this point of view, we estimated the donor–acceptor distance between the rhodanine nucleus and the triazine nucleus in MT1 and MT2. Due to the flexible nature of methylene chain in the systems, it is difficult to estimate the accurate donor–acceptor distance in MT compounds. The average donor–acceptor distance could be estimated statistically by calculating the conformational distribution of these compounds and then by calculating the donor–acceptor distance of each conformers as reported by Yamamoto and co-workers [40,41]. Instead of using those statistical methods, we evaluated the donor–acceptor distance of the linked compound from the most stable conformer which was obtained by searching low-energy conformations by CONFLEX method in CaChe® calculating system.

The most stable conformers thus obtained were shown in Fig. 12. The distance between the rhodanine nucleus of merocyanine and the triazine moiety was estimated from the N(1′), C(1′) atoms in the triazine and S(1), C(1), C(2) atoms in the rhodanine. In the process of electron transfer, it is reasonable to assume that the triazine LUMO π^* orbital would accept electron from the excited dye LUMO orbital to give a triazine anion radical which decompose to a triazine radical and a chloride anion [20,42]. Triazine LUMO π^* and the excited dye LUMO orbitals are located mainly on N(1′), C(1′) atoms in the triazine and S(1), C(1), C(2) atoms in the rhodanine, respectively, as revealed by molecular orbital calculations. Thus, it is reasonable to select those atoms as a measuring point of the donor–acceptor distance. The distance between the rhodanine and the triazine thus obtained was shorter in MT2 than in MT1 (Fig. 12). For example, the distance between N(1′) atom in triazine and C(1) in rhodanine is 12.07 Å in MT1, whereas this value decreases to 9.84 Å in MT2.

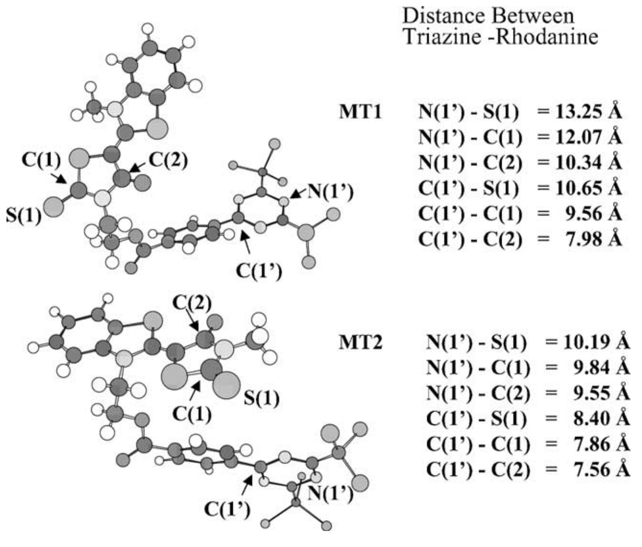

Fig. 12. The most stable conformer of linked-photoinitiators (MT1 and MT2) as calculated by CONFLEX method. *N*-Alkyl substituents of MT1 and MT2 is replaced by *N*-methyl group for simplicity. Donor–acceptor distance between the rhodanine nucleus and the triazine nucleus is also shown.

3.8. The efficiencies of photopolymerization of linked photoinitiating systems

The spectroscopic studies clearly showed that merocyanine-linked initiators exhibit a marked increase in the efficiency of photobleaching and fluorescence quenching than a simple mixture of a dye and an initiator, and that the efficiency among the linked systems is dependent on the numbers and position of methylene units. These results are reasonably explained in terms of the efficiency of electron transfer between the dye and the initiator, which eventually results in the formation of a radical. Thus, it is very important to examine whether a similar trend can be observed when present systems are used as an initiator in real photopolymerization systems.

Thus, the relative efficiency of merocyanine-linked triazines as an initiator in photoinitiating systems of acrylates monomers was evaluated by monitoring the disappearance of the acrylic double bond in the IR absorption. Three merocyanine-linked photoinitiators, MT1, MT2, and MT3 and physical mixtures of merocyanine/triazine were used. It was found that irradiation of acrylic monomer mixtures containing the merocyanine or the triazine alone did not result in polymer formation under our experimental conditions (irradiation at $\lambda = 430$ nm). Fig. 13 shows the kinetics of polymerization employing merocyanine-linked photoinitiators under irradiation. The results clearly showed that the rate is markedly enhanced when the linked photoinitiators were used, as opposed to the unlinked photoinitiator combinations. Among the liked initiators, MT3 is much less effective for photoinitiating polymerization than MT1 and MT2, and MT2 shows larger initiation rate than MT1, although they have the same number of methylene chain. Thus, the trends observed for the polymerization are essentially the same with those observed spectroscopically.

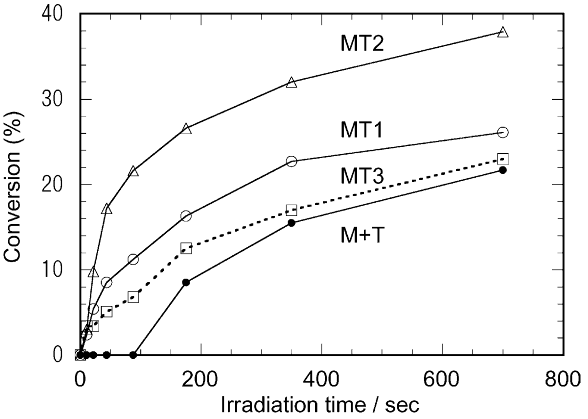

Fig. 13. Conversion (%) of acrylate double bonds as a function of time for polymerization of acrylates containing photoinitiators on irradiation ($\lambda = 430$ nm, intensity $= 34\,\mu W/cm^2$). Photoinitiating system (24 mmol/dm^3); (●) M + T; (○) MT1; (△) MT2; (□) MT3.

4. Conclusions

The photochemical and photophysical processes were examined in a solution and in a photopolymer matrix used in practical photopolymerization systems. The initial reaction step between the photoexcited merocyanine and the triazine was concluded to be electron transfer based on the products analysis and thermodynamic considerations. The active-quenching distance in the matrix was estimated to be about 13 Å.

In the dye-linked photoinitiating systems, the number of methylene unit between the light-absorbing moiety and the radical-generating moiety is demonstrated to be an important factor to control the photochemical reactivity. The linking position is also found to show a slight but distinct effect on the efficiency. Those findings give a clue to develop new dye-linked photoinitiators which are highly sensitive to a visible light.

Acknowledgements

We thank Mr. T. Sorori in our laboratory and Prof. H. Tomioka at Chemistry Department for Materials, Faculty of Engineering, Mie University for helpful discussions. We are also indebted to Dr. K. Hirai at Mie University for mass spectrometric analysis.

References

[1] J.P. Fouassier, Recent Res. Dev. Polym. Sci. 4 (2000) 131.
[2] B.M. Monroe, G.C. Weed, Chem. Rev. 93 (1993) 435.

[3] D.F. Eaton, Adv. Photochem. 13 (1985) 427.
[4] R.S. Davidson, J. Photochem. Photobiol. A: Chem. 73 (1993) 81.
[5] R.S. Davidson, in: J.P. Fouassier, J.F. Rabek (Eds.), Radiation Curing in Polymer Science and Technology, vol. 3, Elsevier, New York, 1993, p. 153.
[6] H. Ito, M. Ishikawa, A. Takada, T. Kudo, Y. Senda, T. Urano, Bull. Chem. Soc. Jpn. 74 (2001) 395.
[7] Y. Tsurutani, H. Ito, M. Ishikawa, T. Urano, J. Photopolym. Sci. Technol. 13 (2000) 83.
[8] H. Ito, T. Urano, S. Nagasaka, S. Shimizu, M. Shimizu, S. Takahara, T. Yamaoka, Bull. Chem. Soc. Jpn. 70 (1997) 1659.
[9] N.J. Turro, Modern Molecular Photochemistry, Benjamin/Cummings, Menlo Park, CA, 1978, p. 316.
[10] G.J. Kavarnos, N.J. Turro, Chem. Rev. 86 (1986) 401.
[11] H. Oevering, M.N. Paddon-Row, M. Heppener, A.M. Oliver, E. Cotsaris, J.W. Verhoeven, N.S. Hush, J. Am. Chem. Soc. 109 (1987) 3258.
[12] K. Kawamura, Japan Patent 2720195 (1990); US Patent 5,262,276 (1993); Chem. Abstr. 112 (1990) 207938.
[13] J.A. Bonham, M.A. Rossman, European Patent 359431 (1990); US Patent 5,034,526 (1991); Chem. Abstr. 113 (1990) 115342.
[14] M. Kohler, J. Ohngemach, European Patent 354458 (1990); Chem. Abstr. 113 (1990) 106437.
[15] F.D. Saeva, D.T. Breslin, European Patent 370693 (1990); Chem. Abstr. 113 (1990) 142293.
[16] B.B. Wright, R.J. DeVoe, European Patent 375160 (1990); Chem. Abstr. 113 (1990) 232255.
[17] D. Burget, F. Amat-Guerri, J.P. Fouassier, R. Mallavia, R. Satre, Acta Polym. 50 (1999) 337.
[18] A. Fimia, R. Sastre, F. Amat-Guerri, R. Mallavia, Macromolecules 27 (1994) 2643.
[19] T. Yamaoka, T. Kageyama, T. Takahashi, T. Urano, J. Photopolym. Sci. Technol. 8 (1995) 1.
[20] G. Pohlers, J.C. Sciano, R. Sinta, R. Brainard, D. Pai, Chem. Mater. 9 (1997) 1353.
[21] G. Pohlers, J.C. Sciano, R. Sinta, E. Step, J. Am. Chem. Soc. 121 (1999) 6167.
[22] C. Grotzinger, D. Burget, P. Jacques, J.P. Fouassier, Macromol. Chem. Phys. 202 (2001) 3513.
[23] G. Buhr, R. Dammel, C.R. Lindley, Polym. Mater. Sci. Eng. 61 (1989) 269.
[24] W. Huimin, J. Yongcai, L. Qingshan, Z. Xiaohong, W. Shikang, J. Appl. Polym. Sci. 84 (2002) 909.
[25] Z. Peng, X. Zhou, S. Carroll, H.J. Geise, B. Peng, R. Dommisse, E. Esmans, R. Carleer, J. Mater. Chem. 6 (1996) 1325.
[26] G. Pawlowski, R. Dammel, K.-J. Przybilla, H. Roschert, W. Spiess, J. Photopolym. Sci. Technol. 4 (1991) 389.
[27] Konisihiroku Photo Ind., Japan Patent 9420 (1965); Chem. Abstr. 63, 18321f.
[28] G.J. Kavarnos, Fundamentals of Photoinduced Electron Transfer, VCH Publishers, New York, 1993.
[29] We could not determine reduction potential of triazine exactly, so we used the value of 2,4,6-tris(trichloromethyl)-1,3,5-triazine reported by Fouassier and co-workers. C. Grotzinger, D. Burget, P. Jacques, J.P. Fouassier, Macromol. Chem. Phys. 202 (2001) 3513.
[30] We could not determined the fluorescence lifetime of merocyanine because of its weak fluorescence intensity. The fluorescence lifetime of merocyanine MC540 was reported to be 0.4 ns. A.C. Brenniston, A. Harriman, C. McAvoy, J. Chem. Soc., Faraday Trans. 94 (1998) 519.
[31] V. Krongauz, J. Phys. Chem. 96 (1992) 2609.
[32] M.A. Ratner, K.V. Mikkelsen, Chem. Rev. 87 (1987) 113.
[33] J.R. Miller, J.V. Beitz, R.K. Huddleston, J. Am. Chem. Soc. 106 (1984) 5057.
[34] K. Nagai, N. Takamiya, M. Kaneko, J. Photochem. Photobiol. A: Chem. 84 (1994) 271.
[35] K. Nagai, J. Tsukamoto, N. Takamiya, M. Kaneko, J. Phys. Chem. 99 (1995) 6648.
[36] H. Ito, T. Urano, S. Nagasaka, A. Takada, H. Kudo, H. Yokoyama, Y. Senda, Bull. Chem. Soc. Jpn. 70 (1997) 2221.
[37] B. Fischer, I.B. Bonte, J. Photochem. 30 (1985) 475.
[38] T. Guarr, M. McGuire, G. McLendon, J. Am. Chem. Soc. 107 (1985) 5104.
[39] J.R. Miller, J. Peeples, M. Schmitt, G.L. Closs, J. Am. Chem. Soc. 104 (1982) 6488.
[40] T. Kanaya, Y. Hatano, M. Yamamoto, Y. Nishijima, Bull. Chem. Soc. Jpn. 52 (1979) 2079.
[41] H. Katayama, S. Ito, M. Yamamoto, J. Phys. Chem. 96 (1992) 10115.
[42] A. Modelli, M. Venuti, L. Szepes, J. Am. Chem. Soc. 124 (2002) 8498.